Magnetic and Mössbauer Study of Cerium-Based Reactive Sorbent

Y. Jiraskova[a,*], J. Bursik[b], O. Zivotsky[c], J. Lunacek[c] and P. Janos[d]

[a]Ceitec IPM, Institute of Physics of Materials, AS CR, Zizkova 22, 616 00 Brno, Czech Republic

[b]Institute of Physics of Materials, AS CR, Zizkova 22, 616 00 Brno, Czech Republic

[c]Department of Physics, VSB-Technical University of Ostrava,
17. listopadu 15, 708 33 Ostrava-Poruba, Czech Republic

[d]Faculty of the Environment, University of Jan Evangelista Purkyne,
Kralova Vysina 7, 400 96 Usti nad Labem, Czech Republic

A new kind of magnetically separable composite consisting initially of magnetite and cerium carbonate nanograins was investigated using magnetic and Mössbauer methods at room and low temperatures. Various stages of calcination treatment in air resulted in a transformation of the cerium carbonate into cerium dioxide and magnetite into more complicated iron oxide compositions. The final CeO_2 nanograins on the surface of α-Fe_2O_3 were obtained after calcination at 973 K.

1. Introduction

Iron oxides nanoparticles, such as magnetite, maghemite and/or hematite, attract still great attention in various technological and industrial applications due to their unique properties [1, 2]. Recently they appear in combination with cerium dioxide for photocatalytic applications [3] or as a magnetically separable reactive sorbent tested for degradation of the organophosphorus pesticide parathion methyl and some chemical warfare agents - nerve gasses, e.g. soman. A reversed-mode co-precipitation of Fe^{3+}/Fe^{2+} salts with aqueous ammonia was used to prepare the magnetite core. Subsequently the magnetite grains were coated with cerium carbonate. The calcination treatment in air has evoked a conversion of the cerium carbonate into cerium oxide, magnetite into maghemite and above 973 K maghemite into hematite [4]. The present paper deals with more detailed analysis of iron oxides after individual steps of calcination using Mössbauer spectrometry.

2. Experimental

Details concerning the preparation of magnetite and subsequently magnetite coated by cerium carbonate as well as a procedure of obtaining magnetic reactive sorbents are described in Ref. [4]. All procedures resulted in a series of samples which are denoted here as ST, where T is the calcination temperature in Kelvins ($473 \leq T \leq 973$). The sample prior calcination is denoted "S0".

Powdered samples for TEM study were treated ultrasonically in an ethanol bath for 5 min and then placed on holey carbon copper grids for observations in an electron microscope Philips CM12 STEM equipped with thermoemission electron source operating at 120 kV.

The magnetic measurements were performed using a Physical Property Measurement System Quantum Design, Inc at room and low temperatures (RT, LT). The hysteresis (HS) curves were taken in magnetic field of ± 4000 kA/m, the field-/zero-field-cooled, FC/ZFC, curves were measured in magnetic field of 8 kA/m.

Mössbauer measurements were carried out at RT and for the selected samples at LT of 5 K in standard transmission geometry using a ^{57}Co(Rh) source. The calibration of velocity scale was performed with α-Fe. All spectra were evaluated within the transmission integral approach using the program CONFIT [5]. In the Mössbauer spectrum the ferromagnetic (fm) phase is represented by sextuplets while the paramagnetic (pm) one by singlets and/or doublets of Lorentzian lines. A weakly resolved atom ordering and/or highly defected region are represented by Gaussian distribution of hyperfine induction. The relative phase representation is denoted by A.

3. Results and discussion

Figure 1 shows TEM micrographs of powders in the as-prepared state, S0, and after various stages of annealing S773, S873, S973. A clear change in morphology of powders is seen after annealing at 873 K and higher. The S0 consists of particles of irregular shapes the size of which ranges from about 5 to 50 nm (Fig. 1a). The annealing up to 773 K did not change the particle size substantially. The better defined smallest particles below 10 nm are seen in the S773 sample (Fig. 1b). The next step of annealing has produced powder with broadened size

———————
*corresponding author; e-mail: jirasko@ipm.cz

distribution (Fig. 1c). The highest annealing temperature of 973 K has contributed to an increase in size and producing well defined rounded particles of hematite and smaller CeO_2 particles on their surfaces (Fig. 1d).
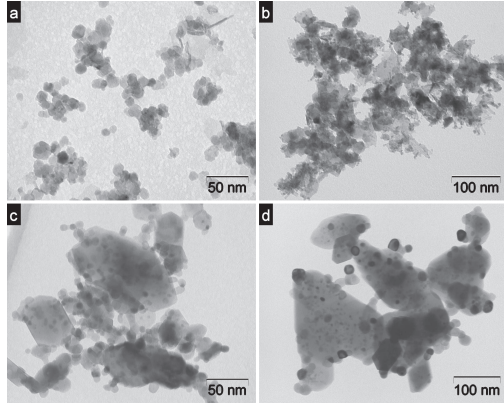

Fig. 1. TEM micrograph of powders in the initial state S0 (a) and after calcination S773 (b), S873 (c), and S973 (d).
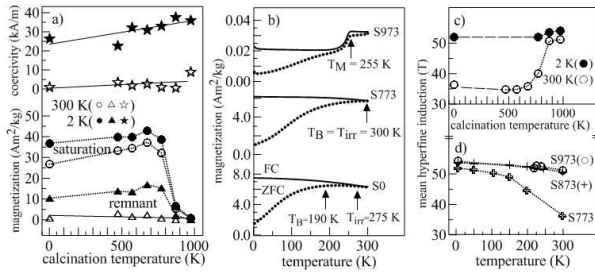

Fig. 2. Changes in magnetic characteristics in dependence on calcination temperature taken from the hysteresis loops with accuracy ±5% (a), FC/ZFC curves for selected samples (b), changes of mean hyperfine induction with calcination temperature (c), and with measuring temperature (d) for selected samples.

The magnetic parameters obtained from the HS curves measured at RT and 2 K (Fig. 2a) show either slightly increasing or nearly constant behavior for both measuring temperatures up to 673 K. The magnetization begins to decrease at the S773 and reaches the lowest value at the S973. This is connected with changes in iron oxide composition as it will be seen from the Mössbauer spectra analysis below. On the other hand the coercivity is influenced predominantly by the particle size. The FC/ZFC magnetization curves (selected seen in Fig. 2b) were used for determination of the blocking, T_B, and irreversible, T_{irr}, temperatures corresponding to a maximum at the ZFC curve and to a point at which both curves separate. The T_B corresponds to most probable particle size in the given ensemble while T_{irr} is a blocking temperature of the largest particles. The difference between them can be taken as quantitative measure of size distribution of particles. Differences T_{irr} - T_B = 59, 62, 59, 51, 0, and

21 K for samples S0 up to S873, respectively, document the similar size distribution of particles up to 573 K. At the sample S773 both T_B and T_{irr} are close to each other reflecting the narrow particle size distribution supporting microscopy observations. The FC/ZFC curves of the S973 sample differ from the previous ones substantially. The temperature T_M in the Fig. 2b agrees well with the Morin transition of hematite [6].
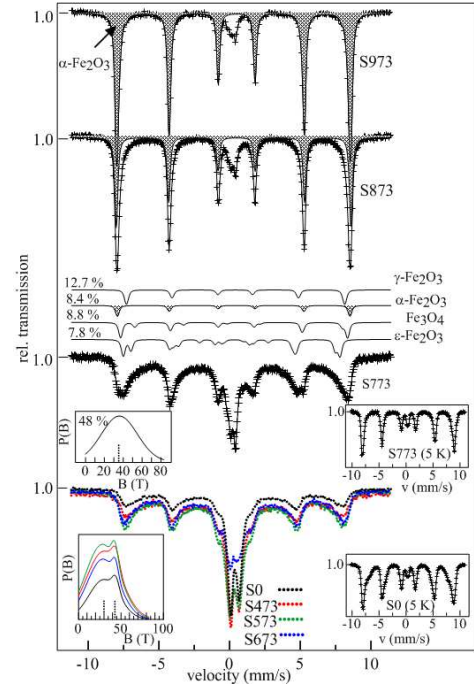

Fig. 3. Mössbauer spectra of the S0 up to S973 samples measured at room temperature. Left insets show the distribution of hyperfine induction, right insets the spectra taken at 5 K.

TABLE I

Mössbauer parameters of the S773 sample measured at 5 K: magnetic induction, B, isomer shift, δ, quadrupole splitting, Δ.

phase	γ-Fe_2O_3	ϵ-Fe_2O_3	α-Fe_2O_3	Fe_3O_4
B [T]	51.6, 48.1	45.9, 51.5	53.9	53.3, 49.7
δ [mm/s]	0.48, 0.41	0.33, 0.25	0.46	0.46, 0.58
Δ [mm/s]	−0.01, 0.00	0.31, 0.02	0.23	−0.17, −0.37

The RT Mössbauer spectra of all samples are seen in Fig. 3. The spectra of the S0 up to S673 samples are very similar and were fitted by two distributions of hyperfine induction with average values at about 30 T and 44 T and by two discrete components with hyperfine parameters corresponding to magnetite; $B_{1,2}$ = 49.2 T, 45.7 T, isomer shift $\delta_{1,2}$ = 0.39 mm/s, 0.58 mm/s, and quadrupole splitting $\Delta_{1,2}$ = −0.02 mm/s, 0.01 mm/s (left insets in Fig. 3). The marked doublet in the middle of spectra consists of three sub-components. The first one ($\sim 6\%$) yields the hyperfine parameters; $\delta = 0.32$ mm/s, $\Delta = 1.05$ mm/s due to the fraction of very small oxide nanoparticles, detected also by TEM, with a super-

paramagnetic behavior. The hyperfine parameters are similar to those published for maghemite nanoparticles in Ref. [7]. This sub-component exists in smaller representation ($\sim 3.2\%$) at the S873 and diminishes at the S973. The next doublet is seen at all samples at RT and LT and its hyperfine parameters ($\delta \sim 0.23$ mm/s and $\Delta \sim 0.35$ mm/s) change only slightly with annealing. It can be speculated that some of the iron resonant atoms are located in the Ce-oxide making it visible by Mössbauer effect and/or that it is a contribution of grain Fe-oxide/Ce-oxide boundaries. The last doublet, $\delta \sim 0.40$ mm/s and $\Delta \sim 0.70$ mm/s, could represent d-positions in β-Fe_2O_3 even if the doublet corresponding to b-positions cannot be resolved in the measured spectra due to its low intensity. Two quadrupole split components represent the crystallographically non-equivalent cation b- and d-positions in the structure [8]. The relative ratio of the fm and pm phases A_{fm}/A_{pm} slightly changes in dependence on treatment temperature for the benefit of fm from 2.17 (S0) to 4.68 (S673). The broad distributions imply that besides the stoichiometric magnetite also nonstoichiometric magnetite containing, e.g., γ-Fe_2O_3 is present. It is known that magnetite transforms into metastable maghemite at lower temperatures because both are of the same crystalline structure. The spectrum of the S773 sample slightly differs. A single distribution had to be used besides discrete sub-components to obtain a proper fit. The discrete sextuplets represent magnetite (9%) and three polymorphous Fe_2O_3 oxides, namely ϵ (8.8%), γ (12.7%), and α (8%) with hyperfine parameters in good agreement with Ref. [6]. No pm β-Fe_2O_3 is present. The spectra of the S873 and S973 are visibly different and consist of discrete six-line components of hematite (S973) accompanied in the S873 sample by small amount of Fe_3O4 (10%), and ϵ-Fe_2O_3 (5%).

The RT Mössbauer results were in some cases supported by LT measurements. The right insets in Fig. 3 show the spectra of the S0 and S773 samples at 5 K. While the magnetite at RT is represented by two components corresponding to Fe^{3+} (tetrahedral sites) and to $Fe^{2.5+}$ (octahedral sites), the LT spectrum has to be fitted with more components for each valence and crystallographic sites. In most studies, the spectra are fitted by five or more components but the exact reason for these components is not fully clear. The six components used here yield magnetic inductions $B = (53.3, 52.3, 51.3, 50.1, 48.5, 46.8)$ T. Different quadrupole splitting values could be due to a complex monoclinic symmetry resulting in an electric field gradient at the cation sites in different sublattices. The values are roughly the same as presented for magnetite nanoparticles at 4.2 K, e.g., in Ref. [9]. Nevertheless, their interpretation would require more detailed discussion. The spectrum analysis of the S773 measured at 5 K has resulted in a set of well resolved discrete sextuplets that could be ascribed to the same Fe-oxide phases as were detected in the RT spectrum but with lower accuracy. The Mössbauer parameters are summarized in Table I.

Similarly, the Fe-oxide phases present at the S873 and S973 at RT were confirmed by LT measurements. Fig. 2c shows the changes of the mean B with calcination temperature obtained from the analysis of spectra measured at 300 K and at 5 K. Contrary to magnetization (Fig. 2a) decreasing with temperature, the opposite is seen for B. The magnetization decreases due to an increasing portion of the weakly ferromagnetic hematite (bulk value 0.3 Am^2kg^{-1}) at the expense of ferrimagnetic magnetite and maghemite present below 673 K. Fig. 2d shows B in dependence on measuring temperature and documents a marked influence of the hematite ($B \sim 54$ T) in the S873 (78%) and S973 (96%).

4. Conclusions

The RT Mössbauer measurements indicated more complex Fe-oxide compositions in the studied Ce-based sorbents. Contrary to Ref. [4] where only maghemite and hematite were detected at 873 K, the Mössbauer analysis of samples calcinated between 773 K and 973 K yielded also the residual magnetite and ϵ-Fe_2O_3 oxide both verified at LT. Pursuant to new results, the changes of the RT and LT macroscopic magnetic characteristics in dependence on calcination temperature could be better explained. The decrease in saturation magnetization above 773 K is caused by increasing portion of the weakly ferromagnetic hematite which simultaneously increases the value of internal magnetic induction.

References

[1] Y.Y. Xu, X.F. Rui, Y.Y. Fu, H. Zhang, *Chem. Phys. Lett.* **410**, 36 (2005).

[2] S.J. Satyawati, R.P. Prajakta, S.N. Madhav, P.P. Bakare, *J. Nanopart. Res.* **8**, 635 (2006).

[3] G.K. Pradhan, K.M. Parida, *Int. J. Eng. Sci. Tech.* **2**, 53 (2010).

[4] P. Janos, P. Kuran, V. Pilarova, J. Trogl, M. Stastny, O. Pelant, J. Henych, S. Bakardjieva, O. Zivotsky, M. Kormunda, K. Mazanec, *Chem. Eng. J.* **262**, 747 (2015).

[5] T. Zak, Y. Jiraskova, *Surf. Interface Anal.* **38**, 710 (2006).

[6] R.M. Cornell, U. Schwertmann, in: *The Iron Oxides*, Wiley-VCH, Weinheim 2003, p. 117.

[7] R. Zboril, M. Mashlan, K. Barcova, M. Vujtek, *Hyperfine Interact.* **139-140**, 597 (2002).

[8] R. Zboril, M. Mashlan, D. Petridis, *Chem. Mater.* **14**, 969 (2002).

[9] I. Dezsi, Cs. Fetzer, Á. Gombkötö, I. Szücs, J. Gubicza, T. Ungár, *J. Appl. Phys.* **103**, 104312 (2008).